03

# Numerical investigation of the effect of tangential helium injection on the linear stability of a compressible boundary layer on a flat plate

© I.S. Matveev, S.O. Morozov, S.V. Lukashevich, A.N. Shiplyuk

Khristianovich Institute of Theoretical and Applied Mechanics, Siberian Branch, Russian Academy of Sciences,

Novosibirsk, Russia

e-mail: i.matveev@g.nsu.ru

Received November 12, 2024 Revised March 24, 2025

Revised March 24, 2025 Accepted March 24, 2025

The paper is devoted to the numerical investigation of the effect of the geometry of a single channel for tangential helium injection on disturbances in a compressible boundary layer. The boundary layer calculations are performed within the framework of the Navier-Stokes equations in a two-dimensional plane formulation for compressible flows. The boundary layer stability calculations are carried out within the framework of the linear stability theory in the locally parallel approximation taking into account a binary gas mixture. It is shown that, regardless of the configuration of a single channel, the introduction of helium into the boundary layer stabilizes disturbances of the second mode and destabilizes disturbances of the first mode in the region close to the injection site. However, at a sufficient distance from the gas injection site, the growth rates of two-dimensional disturbances of the first and second Mack modes are less than in the case without injection. It is also shown that, at a constant mass flow rate, the channel geometry mainly affects the boundary layer stability only in the helium injection region. An increase in the channel height leads to an increase in the growth rates of the two-dimensional disturbances of the second mode and a decrease in the growth rates of the two-dimensional disturbances of the first mode.

Keywords: boundary layer, linear theory of stability, first Mack mode, second Mack mode, boundary layer stabilization

DOI: 10.61011/TP.2025.07.61445.456-24

## Introduction

It is known that scenarios of a laminar-turbulent transition of a boundary layer can differ depending on roughness of the surface and a level of disturbances of the oncoming stream. One of the scenarios describes development of disturbances in an supersonic boundary layer with required smallness of disturbances and roughness of the surface [1]. The said scenario of the transition consists of a receptivity phase, a linear and a nonlinear phase of development of disturbances in the boundary layer. The present paper deals with the linear phase of development of disturbances. As shown in the studies [2,3], in the linear stage, the most progressing disturbances in a two-dimensional compressible boundary layer are disturbances of the first and the second mode according to the Mack classification. Methods of stabilization of disturbances of the first and second modes substantially differ [3,4].

The first mode can be stabilized by using surface mass exchange [5], sublimating coatings [6], cooling of the surface [3] or injection of a heavy gas into the boundary layer [7]. The second mode can be stabilized by using porous coatings [8–10], wavy surfaces [11,12], heating of the surface in a disturbance progressing area [13], local heating or cooling to the disturbance progressing area [14], surface local mass exchange [15], and injection of a light gas [16,17]. The paper [18] has investigated three methods of blowing the gas into the boundary layer: through the system of slits arranged at an angle to the surface, through the porous

surface and through the perforated insert. It is shown that all the three methods effectively reduce a growth rate of disturbances of the first mode in the boundary layer with injection of the heavy gas.

The aim of the present study is to investigate influence of helium injection through a single channel on stability of the boundary layer on the flat plate with the Mach number of 4

## Calculation procedure

The flow is simulated in the AnsysFluent software. The performed studies are based on computational modeling within the framework of the Navier-Stokes equations in a two-dimensional plane formulation for compressible flows. A stationary problem for a laminar flow of the two-component gas (air+helium) is solved. Fig. 1 schematically

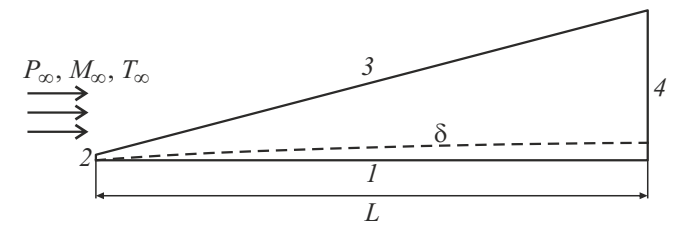


**Figure 1.** Schematic diagram of a calculation area: I — the surface, 2, 3 — the inlet limit, 4 — the output limit,  $\delta$  — the limit of the boundary layer.

15\* 1187

show the calculation area. The lower limit I has a wall with no-slip condition and the constant temperature pre-defined. The inlet of the main air flow (the boundaries 2 and 3) has a "pressure-far-field" boundary condition with the Mach number of 4 pre-defined. The Reynolds number along the plate length is  $Re_L = 2 \cdot 10^6$ . The temperature factor  $\frac{T_w^*}{T_0}=0.8$ , where  $T_w^*$  — the surface temperature,  $T_0^*$  — the stagnation temperature. The temperature of the oncoming stream — 70 K. The limit 4 has a "pressure-outlet" condition pre-defined. The inlet of an injection channel (the limit 5 of Fig. 2) has a "mass-flow-inlet" boundary condition at a constant mass flow rate of helium set. The air parameters are determined by the following laws: thermal conductivity as per the kinetic theory, viscosity as per Sutherland Thermal conductivity and viscosity of helium are determined as per the kinetic theory. Thermal conductivity and viscosity of the two-component mixture of the gases are calculated as per the law of mixing of an ideal gas. In the same approximations for the binary mixture of the gases, numerical studies are performed in the paper [7,18], which describes it with more details.

Stability of the boundary layer has been calculated within the framework of the linear stability theory in a localparallel approximation with taking into account the binary mixture of gases [7,18]. The eigenproblem was solved by a collocation method [19,20].

The below-given results of the numerical study are provided in a dimensionless form. The density  $\rho^*$  and the longitudinal velocity  $U^*$  are rated to corresponding parameters of the oncoming stream  $\rho_{\infty}^*$  and  $U_{\infty}^*$ . The dimensionless longitudinal coordinate is determined as  $x = x^*/L^*$ , where  $x^*$  — the dimensional coordinate,  $L^*$  the length of the plate, the dimensionless surface-normal coordinate  $y(x) = y^*/\delta^*(x)$  — where  $y^*$  — the dimensional coordinate,  $\delta^*(x)$  — the thickness of the boundary layer, which depends on the longitudinal coordinate x. The growth rate —  $\alpha_i$  and the frequency  $\omega$  of disturbances are rated as follows:  $-\alpha_i = -\alpha_i^* L^*$  and  $\omega = 2\pi f^* \delta^* / U_{\infty}^*$ , where  $\alpha_i^*$  the dimensional degree of growth along the coordinate x, and  $f^*$  — the dimensional frequency of disturbances. The thickness of the boundary layer  $\delta^*$  was determined by the coordinate, at which the parameter  $\rho^* \frac{dU^*}{dy^*}$  was 1% of the maximum value.

The studied model is a flat plate that is arranged at the zero incidence angle. For better convergence of the

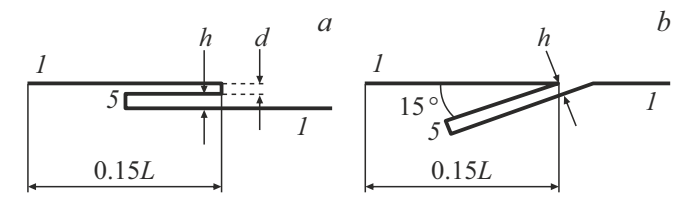


**Figure 2.** Schematic diagram of the studied model in the gas injection region with a channel that is parallel to the plate (a) and at the angle of  $15^{\circ}$  (b). I — the surface, 5 — the inlet of the injection channel.

solution of the two-dimensional problem with the stationary boundary layer of the two-component mixture, helium was injected through an elongated channel, so that the "mass-flow-inlet" boundary condition was out of an area of interaction with the main stream (Fig. 2). It considered an arrangement of the injection channel in parallel to the plate (Fig. 2, a) and at the angle of 15° Fig. 2, b). The edge of the gas injection channel is arranged at the distance x = 0.15from the leading edge of the plate. The dimensionless height of the channel is  $h=h^*/\delta_{0.15}^*=0.08$  , 0.15, 0.3, where  $\delta_{0.15}^*$  — the thickness of the boundary layer on the flat plate without the injection channel (the basic case) when x = 0.15. The dimensionless height of the channel edge d is invariable and is  $d^*/\delta_{0.15}^*=0.1$ . The height of the channel that is arranged at the angle is h = 0.15. Unlike a configuration with the parallel channel, the angular configuration has no backward-facing step. The studies are performed for the rated mass flow rate of helium q within the range from  $4 \cdot 10^{-3}$  to  $16 \cdot 10^{-3}$ . It is rated to a value of the mass flow rate of air transmitted through a cross section of the boundary layer when x = 0.15. The temperature of the injected gas is equal to the temperature of the surface.

In order to perform the calculation, a structured two-dimensional grid is constructed. The calculation grid consists of two subregions: an area of the main stream and an area of the boundary layer. The dashed line of Fig. 1 is an upper boundary of the boundary layer ( $\delta$ ). In the boundary layer, the grid cells are orthogonal to the surface. The number of the cells per the thickness of the boundary layer is still the same along the plate. In order to reduce numerical oscillations, the grid cells in the upper part of the calculation area are arranged along a surge of compaction. For this, the position of the surge of compaction is determined from preliminary calculations. The upper limit of the calculation area 3 is constructed upstream in parallel to the surge The grid is denser towards

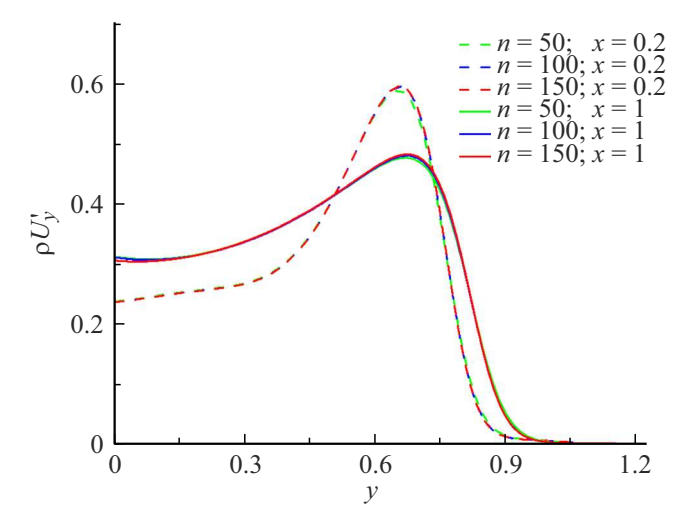


**Figure 3.** Dependence of the parameter  $\rho \frac{dU}{dy}$  on the surface-normal coordinate y with the channel that is parallel to the plate and has a height h = 0.15 and at the mass flow rate of helium  $q = 8 \cdot 10^{-3}$ .

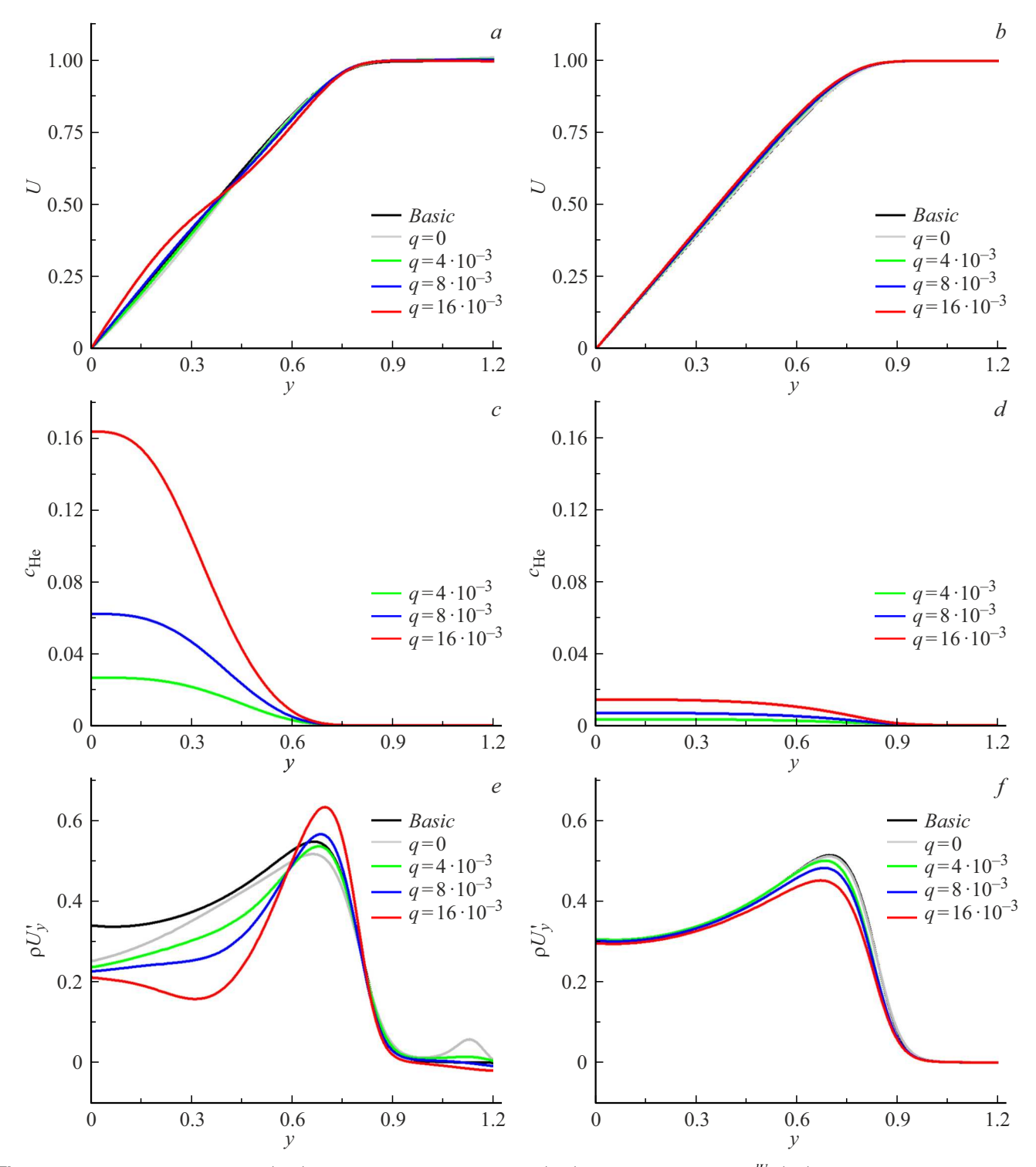


**Figure 4.** Profiles of the velocity (a,b), the mass fraction of helium (c,d) and the parameter  $\rho \frac{dU}{dy}$  (e,f) in the boundary layer for the plate-parallel channel of the height h=0.15 when x=0.2 (a,c,e) and x=1 (b,d,f).

the forward edge of the plate, the gas injection channel, the surge and towards the upper limit of the boundary layer in accordance with a monotonic rational quadratic spline (MRQS), which makes it possible to create smooth distribution of grid dots with a guarantee of monotony of this distribution [21].

Convergence along the grids is studied. The convergence is studied by the parameter  $\rho \frac{dU}{dy}$ , using this parameter, it is possible to judge the presence of instability in the boundary layer. Fig. 3 shows the grid convergence as exemplified by the boundary layer in case of parallel injection through the channel of the height h=0.15 when  $q=8\cdot 10^{-3}$ . The

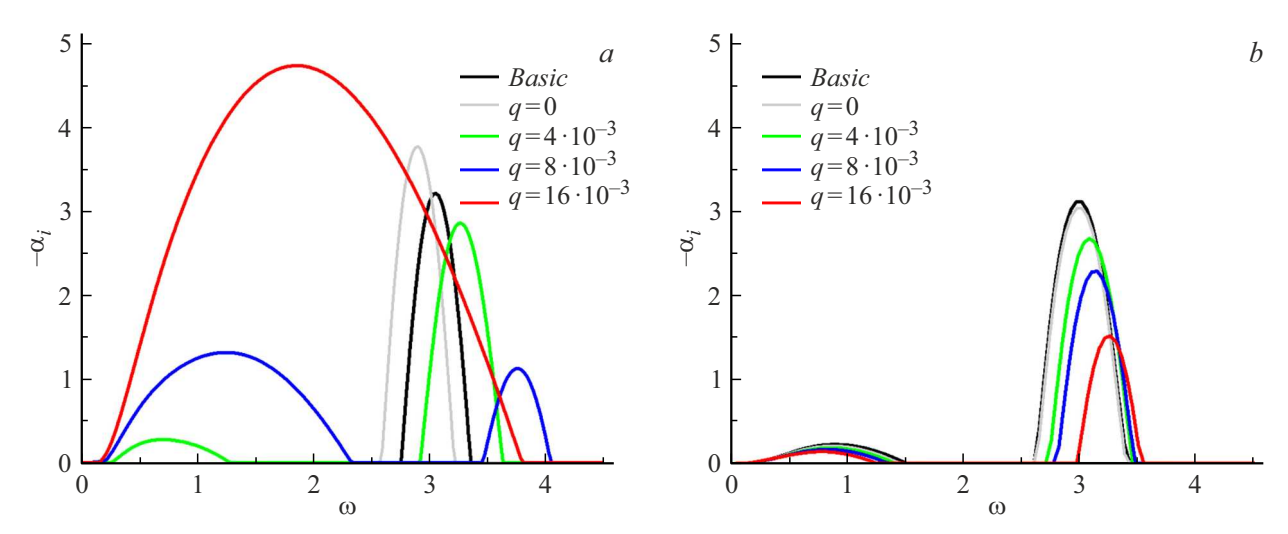


**Figure 5.** Dependence of the growth rates on the frequency of disturbances for the plate-parallel channel of the height h = 0.15 when x = 0.2 (a) and x = 1 (b).

number of the cells per the boundary layer is n = 50, 100, 150. The maximum relative deviation of the parameter  $\rho \frac{dU}{dy}$  between all the considered cases is 1.4%. The further study was on the calculation grid with n = 100.

#### 2. Results

We have simulated stationary supersonic flow around the flat plate at the zero incidence angle with injection of helium into the boundary layer within the range of mass flow rates from  $4 \cdot 10^{-3}$  to  $16 \cdot 10^{-3}$ . Fig. 4 shows the dimensionless profiles of the velocity U(a,b), the mass fraction of helium  $c_{\text{He}}(c,d)$  and the parameter  $\rho \frac{dU}{dv}(e,f)$  in the boundary layer when x = 0.2 (a, c, e) and x = 1 (b, d, f)for the various configurations of the injections helium. The results are given for the plate-parallel channel with the height h = 0.15. The range of the mass flow rates is limited by the value  $q = 16 \cdot 10^{-3}$ , as when  $q \ge 16 \cdot 10^{-3}$  the profile of the velocity of the boundary layer in the helium injection region is distorted (Fig. 4, a), and an additional inflection point appears on the profile  $\rho \frac{dU}{dv}$  (Fig. 4, e), thereby affecting stability of the boundary layer. When  $q \ge 16 \cdot 10^{-3}$ , the velocity of supplied helium at the channel outlet exceeds the velocity of the oncoming stream and the local speed of sound. When x = 1 and  $q = 16 \cdot 10^{-3}$ , the profile of the velocity of the boundary layer is aligned and has a relatively small difference with the profiles when  $q = (4, 8) \cdot 10^{-3}$  (Fig. 4, b). The profiles of the boundary layer when x = 1 are qualitatively similar by the parameter  $\rho \frac{dU}{dv}$ , but the difference of their maximums reaches 14.4% (Fig. 4, f). Besides, in Fig. 4, e, at the coordinate y > 1there are distortions of the parameter  $\rho \frac{dU}{dv}$ ; these distortions are caused by the weak shock wave, which is created by the injection channel. Fig. 4, c, d shows the profiles of helium concentration. It is clear that when x = 0.2 the main portion of helium is contained in the lower half of the boundary layer y < 0.5, whereas when x = 1 helium is almost uniformly distributed along the entire boundary layer. Influence of the step was determined by calculating the boundary layer without helium injection (q = 0). It is shown that when x = 0.2 the profiles of the velocity U (Fig. 4, a) and the parameter  $\rho \frac{dU}{dy}$  (Fig. 4, e) are quite strongly distorted in relation to the basic case (without the channel). When x = 1, the influence of the step on the profiles and the dimensional thickness  $\delta^*$  of the boundary layer is small

The obtained results of computational modeling of the stationary boundary layer were used to calculate the growth rates of the unstable two-dimensional disturbances within the framework of the linear stability theory in the cross sections x = 0.2 (Fig. 5, a) and x = 1 (Fig. 5, b) for various values of the mass flow rate of injected helium. The dependences of the growth rates on the frequency of disturbances are shown for the configuration with the plateparallel gas injection channel of the height h = 0.15. It can be seen from Fig. 5, a that in the helium injection region the growth rates of the second mode become less than in the case without injection, so for the first mode do higher. With increase of the mass flow rate, the growth rates of the second mode decrease, while the growth rates of the first mode increase. With the mass flow rate  $q = 16 \cdot 10^{-3}$ , no unstable disturbance corresponding to the second mode is observed. The increase of the mass flow rate of helium results in increase of the first mode. When  $q = 16 \cdot 10^{-3}$ , the first mode of disturbances begins to dominate over the second mode, while the frequency range is extended to capture the frequencies that are typical for the second mode of disturbances. Further downstream, with increase of the mass flow rate of helium, there is a decrease of the growth rates of not only the second mode, but of the first one as well. It can also be seen from Fig. 5 that with increase of the mass flow rate the area of the progressing disturbances of the second mode is shifted towards the higher frequencies.

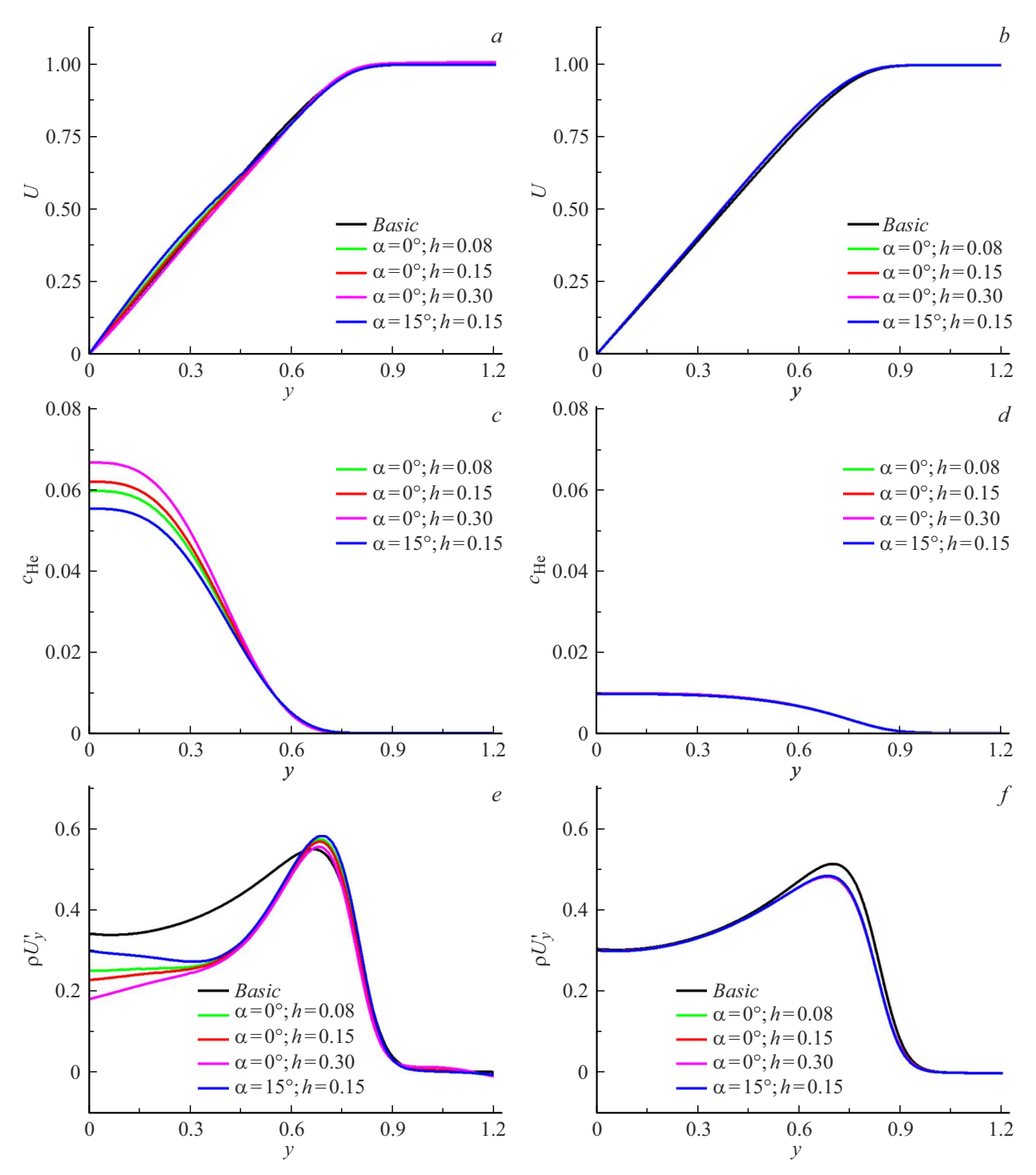


**Figure 6.** Dependence of the velocity (a, b), the mass fraction of helium (c, d) and the parameter  $\rho \frac{dU}{dy}$  (e, f) on the surface-formal coordinate y when x = 0.2 (a, c, e) and x = 1 (b, d, f) for  $q = 8 \cdot 10^{-3}$ .

Without injection (q = 0), the availability of the channel step results in increase of the growth rates of the second mode of disturbances when x = 0.2 in comparison with the basic case and has almost no effect on the growth rates when x = 1.

Fig. 6 shows the dimensionless profiles of the velocity U(a,b), the mass fraction of helium  $c_{\rm He}(c,d)$  and the parameter  $\rho \frac{dU}{dv}(e,f)$  in the boundary layer when x=0.2

(a, c, e) and x = 1 (b, d, f) for the various configurations of the injected channel. The results of the calculations are given for the mass flow rate of helium  $q = 8 \cdot 10^{-3}$ . It is clear from Fig. 6, a that in the area close to the channel when x = 0.2 arranged at the angle, the profile of the boundary layer is distorted in relation to the other geometries, as the rate of helium injection has a higher normal component than for parallel injection. It is also clear from Fig. 6, e that

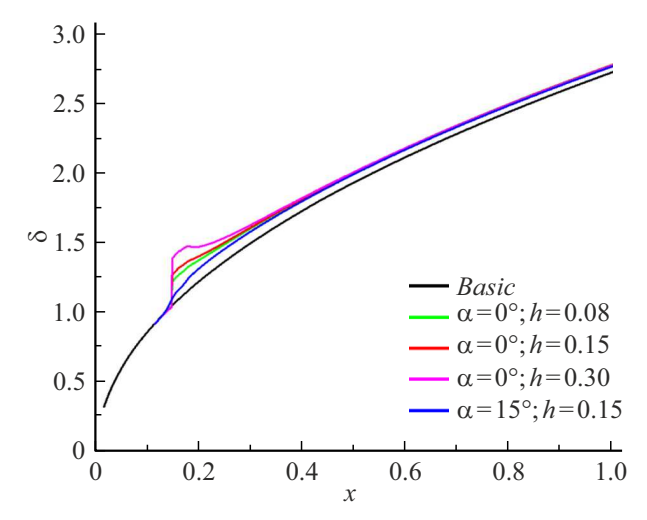


**Figure 7.** Dependence of the thickness of the boundary layer  $\delta$  on the longitudinal coordinate x for the various configurations of the channel for  $q = 8 \cdot 10^{-3}$ .

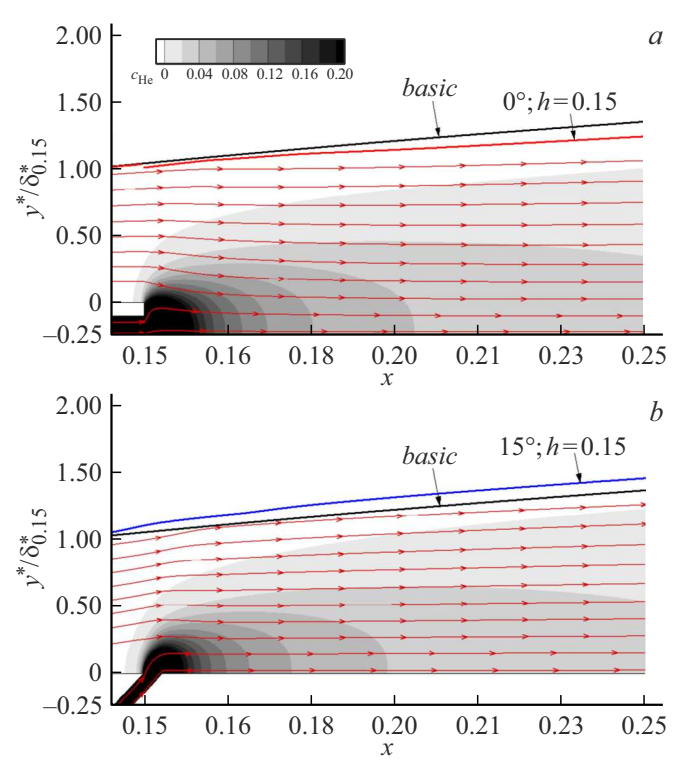
the geometry of the channel to a greater extent affects the profile of the boundary layer when y < 0.4. With increase of the channel height, the helium concentration  $c_{\rm He}$  near the surface increases (Fig. 6, c). At a sufficient distance from the injection site, the channel geometry slightly affects the profile of the boundary layer, therefore, the graphs are almost aligned in one line. It can be seen on Fig. 6, b, d, f) for x = 1. Thus, it is seen that helium is distributed along the boundary layer almost equally at all the studied geometries (Fig. 6, d).

Fig. 7 shows the dependence of the dimensionless thickness of the boundary layer  $\delta = \delta^*/\delta_{0.15}^*$  the longitudinal coordinate x for the cases shown on Fig. 6. As there is the step in parallel injection, then the thickness of the boundary layer is counted from a new surface, and there is a sharp increase of the thickness of the boundary layer in Fig. 7 around x = 0.15. In the case with injection at the angle, there is no step, and the thickness of the boundary layer begins to differ from the case without injection upstream of the edge of the injecting channel (Fig. 2), which is due to a positive pressure gradient in this area. It is clear that for the case of parallel injection the increased thickness of the boundary layer is mainly contributed by the availability of the step. The influence of the channel geometry on the boundary layer decreases downstream, and when x > 0.4the differences in the thickness of the boundary layer are below 1% at the fixed mass flow rate of helium. It should be noted that this coordinate corresponds to  $60\delta_{0.15}^*$ , and therefore we should have expected such an effect from the channels, whose size is less than the thickness of the boundary layer.

Fig. 8 shows contours of helium concentration in the area close to the injection channel for the case of parallel injection with the channel h=0.15 (Fig. 8, a) and for the case with angular injection (Fig. 8, b) when  $q=8\cdot 10^{-3}$ . The arrow lines denote the stream line, while the solid

lines denote the boundary layer edge for the basic case and for the case with injection. It can be seen that when  $q = 8 \cdot 10^{-3}$ , injection of helium shifts a physical position of the limit of the boundary layer for no more than 6 %. The flow lines of parallel injection (Fig. 8, a) after the channel edge when x = 0.15 are directed to the surface, and then its direction smoothly transits to a direction that is typical for the boundary layer on the flat plate. For the angular configuration, injection results in increase of an inclination angle of the flow line in relation of the surface in the injection region. In general, it can be seen that injection in the studied range of the flow rates slightly deforms the profiles of the velocity, whereas the changes mainly concern the density, the viscosity, thermal conductivity and heat capacity due to a significant difference in a molar mass of air and helium.

Besides, based on the results of computational modeling of the stationary boundary layer within the framework of the linear stability theory we have obtained the growth rates  $-\alpha_i$  of the unstable two-dimensional disturbances when x=0.2 (Fig. 9, a) and x=1 (Fig. 9, b) at the mass flow rate of helium  $q=8\cdot 10^{-3}$  for the various configurations of the channels. It can be seen from Fig. 9, a that the configuration with the channel arranged at the angle of 15 ° and of the height h=0.15 almost completely suppresses the second mode of the unstable disturbances when x=0.2 (up to 95%), but significantly destabilizes the first mode in relation



**Figure 8.** Contours of helium concentration in the injection region. The arrow lines — the flow lines, the solid lines — the limit of the boundary layer for the basic case and for the case with injection; a — parallel injection with h=0.15, b — injection at the angle of 15  $^{\circ}$  with h=0.15.

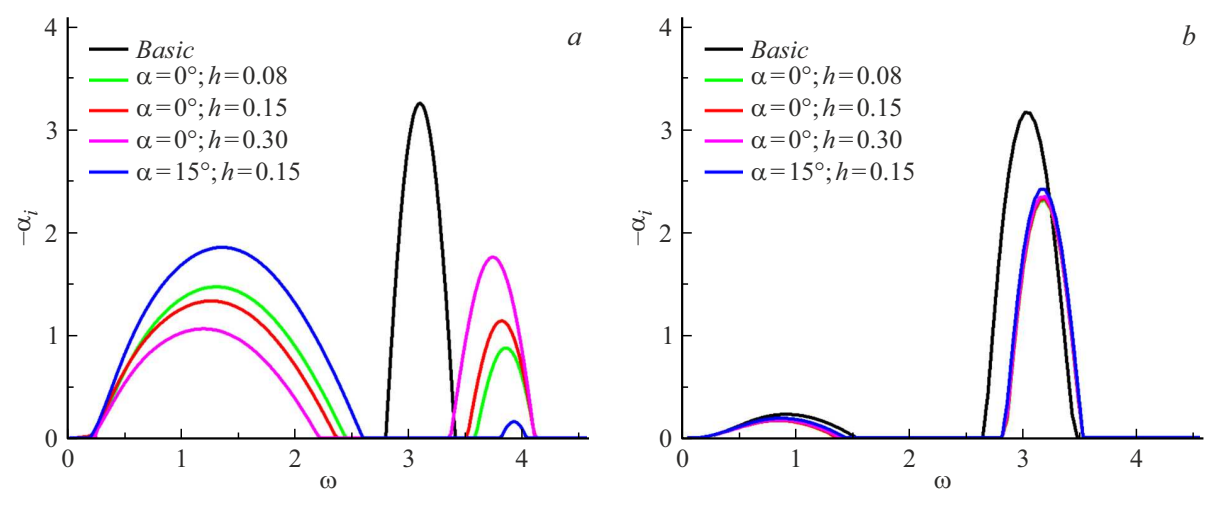


**Figure 9.** Dependence of the growth rates on the frequency with the mass flow rate  $q = 8 \cdot 10^{-3}$  for x = 0.2 (a) and x = 1 (b).

to the other geometries. It can be seen from Fig. 9, a that by changing the channel height it is possible to vary the growth rates of disturbances of the first and the second mode. The substantial difference in the growth rates for the angular channel with the case of the parallel channel can be related to the availability of the back-ward-facing step in the last case. As shown in Fig. 5, a, the availability of the step without helium injection results in a substantial increase of the growth rates of the second mode, while in the presence of helium the growth rates become less than in the basic case. Thus, when x = 0.2 injection of helium with parallel arrangement of the channel affects the step-distorted boundary layer, and, probably, it resulted in a significant difference in the growth rates with the case of angular injection.

The growth rates of the second mode of disturbances are directly proportional to the height of the helium injection channel. When x=1, due to a small difference of the profiles of the boundary layer at the various configurations (Fig. 6), the growth rates of disturbances slightly differ as well. The relative change is below 5%.

As it is known, for disturbances of the first Mack mode, the growth rates of the three-dimensional disturbances are higher than those of the two-dimensional ones for the boundary layer on the flat plate. It was found during this study that in terms of quality influence of injection of helium and the channel geometry turns out to be the same as in the case for the two-dimensional disturbances. Increase of the mass flow rate of helium or decrease of the channel height destabilizes disturbances of the first mode in the gas injection region and stabilizes disturbances of the first mode at a sufficient distance from the injection channel.

### Conclusion

We have studied the influence of helium injection through the single channel on stability of the boundary layer on the flat plate with the Mach number of 4. The study also included consideration of the influence of the mass flow rate and the geometry of the single channel for tangential helium injection on the two-dimensional disturbances of the first and the second Mack modes within the framework of the linear stability theory.

It is shown that helium injection through the single channel stabilizes the two-dimensional disturbances of the first and the second mode at a sufficient distance from the injection site and this effect amplifies with increase of the mass flow rate of the gas. However, in the area close to the channel increase of the mass flow rate of helium destabilizes disturbances of the first mode. The growth rates of the second mode of disturbances in the injection region decrease with reduction of the channel height, while those for the first mode increase. By changing the channel height, it is possible to achieve the effect, at which the growth rates of the two-dimensional disturbances of the first and the second mode in the injection region will not exceed the growth rate of disturbances in the case without injection. It is shown that at a sufficient distance from the injection site the channel geometry slightly affects the profile of the boundary layer, as a result of which the growth rates of disturbances slightly differ.

#### **Funding**

The study was carried out under the state assignment by RAS SB ITAM (state registration number: 124020900037-2)

## **Conflict of interest**

The authors declare that they have no conflict of interest.

#### References

 M.V. Morkovin, E. Reshotko, T. Herbert. Bull. APS, 39 (9), 1 (1994).

- [2] L.M. Mack. AIAA J., 13 (3), 278 (1975).DOI: 10.2514/3.49693
- [3] S.A. Gaponov, A.A. Maslov. Razvitie vozmushchenii v szhimaemykh potokakh (Nauka, Novosibirsk, 1980) (in Russian).
- [4] A. Fedorov. Ann. Rev. Fluid Mech., 43, 79 (2011).DOI: 10.1146/annurev-fluid-122109-160750
- [5] S.A. Gaponov, N.M. Terekhova. Thermophys. Aeromechan., 19 (2), 209 (2012). DOI: 10.1134/S0869864312020059
- [6] S.A. Gaponov, B.V. Smorodsky. Thermophys. Aeromechan., 27 (2), 205 (2020). DOI: 10.1134/S0869864320020043
- [7] S.A.Gaponov, Yu.G. Ermolaev, N.N. Zubkov, A.D. Kosinov,
   V.I. Lysenko, B.V. Smorodskii, A.A. Yatskikh. Fluid Dynamics, 52 (6), 769 (2017). DOI: 10.1134/S0015462817060052
- [8] V.M. Fomin, F.V. Fedorov, V.F. Kozlov, A.N. Shiplyuk, A.A. Maslov, E.V. Burov, N.D. Malmuth. Dokl. Phys., 49 (12), 763 (2004). DOI: 10.1134/1.1848635
- [9] S.O.Morozov, S.V. Lukashevich, V.G. Soudakov,
   A.N. Shiplyuk. Thermophys. Aeromechan., 25 (6), 793 (2018). DOI: 10.1134/S086986431806001X
- [10] S.V. Lukashevich, S.O. Morozov, A.N. Shiplyuk. Tech. Phys. Lett., 38'(12), 1077 (2012).
   DOI: 10.1134/S1063785012120073
- [11] D.A. Bountin, A.A. Maslov. Tech. Phys. Lett., 43 (7), 623 (2017). DOI: 10.1134/S1063785017070021
- [12] A.V. Fedorov, A.V. Novikov, N.N. Semenov. Int. J. Fluid Mechan. Res., 47 (4), 329 (2020).
   DOI: 10.1615/InterJFluidMechRes.2020033001
- [13] A.V. Fedorov, V. Soudakov, I. Egorov, A.A. Sidorenko, Y.V. Gromyko, D.A. Bountin, P.A. Polivanov, A.A. Maslov. AIAA J., 53 (9), 2512 (2015). DOI: 10.2514/1.J053666
- [14] D.A. Buntin, A.A. Maslov, Y.V. Gromyko. Tech. Phys. Lett.,43 (10), 916 (2017). DOI: 10.1134/S1063785017100194
- [15] A.V. Novikov, A.O. Obraz, D.A. Timokhin. Fluid Dynam., 58, 232 (2023). DOI: 10.1134/S001546282260184X
- [16] F. MiróMiró, F. Pinna. J. Fluid Mech., 890, 1 (2020). DOI: 10.1017/jfm.2020.804
- [17] S.O. Morozov, B.V. Smorodskii, A.N. Shiplyuk. *Tez. dokl. XVII Vserossiiskii seminar s mezhdunarodnym uchastiem: dinamika mnogofaznykh sred* (Novosibirsk, Rossiya, 2021), s. 91 (in Russian).
- [18] V.I. Lysenko, S.A. Gaponov, B.A. Smorodsky, Y.G. Yermolaev, A.D. Kosinov. Phys. Fluids, 31 (10), 104103 (2019). DOI: 10.1063/1.5112145
- [19] A.V. Boiko, K.V. Demyanko, Y.M. Nechepurenko. Russ. J. Numerical Analysis and Mathematical Modelling, 32 (1), 1 (2017). DOI: 10.1515/rnam-2017-0001
- [20] M.R. Malik. J. Comp. Phys., 86 (2), 376 (1990).DOI: 10.1016/0021-9991(90)90106-B
- [21] J. Samareh-Abolhassani, I. Sadrehaghighi, R.E. Smith, S.N. Ti-wari. J. Aircraft, 27 (10), 873 (1990).
  DOI: 10.2514/3.45951

Translated by M.Shevelev